Malaysian Journal of Chemistry, 2022, Vol. 24(2), 12-23
(Special Issue: *2nd IKM Pahang Branch Symposium 2022 – Sustainability & Diversity Through Chemistry*)

Eggshell Membrane Functionalized with Waste Palm Cooking Oil for Removal of Alizarin Red from Aqueous Solutions

Siti Khalijah Mahmad Rozi[1], Anis Atikah Mohd Zulkifle[1], Ahmad Razali Ishak[2*], Fairuz Liyana Mohd Rasdi[2], Nazri Che Dom[2], Nurul Yani Rahim[3], Mohd Yusmaidie Aziz[4] and Siti Rohana Mohd Yatim[2]

[1]Faculty of Chemical Engineering Technology, Universiti Malaysia Perlis, 02600 Arau, Perlis
[2]Centre for Environmental Health and Safety, Faculty of Health Sciences, Universiti Teknologi MARA, Puncak Alam Campus, 42300 Kuala Selangor, Malaysia
[3]School of Chemical Sciences, Universiti Sains Malaysia, 11900 Minden, Pulau Pinang
[4]Integrative Medicine Cluster, Advanced Medical and Dental Institute, Universiti Sains Malaysia, 13200 Bertam, Kepala Batas, Penang, Malaysia
*Corresponding author (e-mail: ahmadr2772@uitm.edu.my)

Eggshell membrane (ESM) was functionalized with waste palm cooking oil (WPCO) and used as an adsorbent (ESM@WPCO) for the removal of toxic Alizarin Red dye from aqueous solutions. SEM analysis of ESM@WPCO revealed a large microporous network of interwoven and coalescing shell membrane fibres. FTIR analysis confirmed the attachment of free fatty acids onto the surface of ESM. The protocol for Alizarin Red removal using ESM@WPCO was optimized for pH, adsorbent dosage, contact time and initial concentration. A maximum removal rate of 93% was achieved at pH 2, with an adsorbent dosage of 20 mg for 50 mg L^{-1} Alizarin Red, and a treatment time of 40 min. The adsorption isotherms were also analysed using Langmuir and Freundlich models, and it was found that the Freundlich model was better in describing the adsorption isotherm process, with an R^2 value of 0.98. From this model, a maximum adsorption capacity (K_f) value of 8.41 mg g^{-1} was obtained. The adsorption kinetics followed a pseudo-second order model with an R^2 value of 0.99. The results also revealed that ESM@WPCO was an effective adsorbent for the removal of Alizarin Red from aqueous solutions.

Key words: Eggshell membrane; waste palm cooking oil; free fatty acids; Alizarin Red

Received: December 2021; Accepted: February 2022

Dye-containing wastewater is a serious environmental threat to aquatic life and human beings due to its toxic, carcinogenic, mutagenic, and teratogenic properties. Untreated dye discharged into water bodies also causes turbidity, which retards the photosynthesis process of plankton and algae, and this can disrupt the food chain. Industries that deal with dyes, textile ennoblement, food colouring, cosmetics, printing, carpets, and leather manufacturing contribute to the discharge of dye effluents [1–3]. The dyestuff industry alone is responsible for up to 20% of all industrial water pollution [4]. Dye-containing wastewater must be treated before it is discharged into water bodies. Unfortunately, dyes are notoriously difficult to remove due to their persistence and non-biodegradable nature.

Dyes are colourants that are used to impart colour onto other substances. There are two types of dyes, natural and synthetic. Synthetic dyes are commonly used in industry because they are cheap, available in a wide range of colours and possess a strong binding affinity towards fibres [5,6]. These dyes can be categorized into groups such as azo, anthraquinone, sulfur, phthalocyanine, and triarylmethane, based on their chemical structure [7]. Alizarin Red (AR) is one of the most long-lasting anthraquinone dyes as it is resistant to chemical, physical, and biological degradation [8]. Despite its carcinogenic and mutagenic properties, this anionic dye is widely used in the textile industry to colour woven fabrics, wool and cotton [9]. The strong physicochemical, thermal, and optical stability of AR is due to its complex fused aromatic structure, which makes it resistant to degradation [10]. Hence, considerable effort has been expended to find efficient methods for the removal of AR from wastewater before its discharge into water bodies.

There are several strategies for the treatment of wastewater dyes including biodegradation methods (fungi, algae, bacteria, and microbial fuel cells), chemical methods (photocatalytic oxidation, ozone treatment, and Fenton's process), and physicochemical methods (adsorption, ion exchange, coagulation, and filtration) [11]. Among these strategies, adsorption is the most straightforward, efficient, and cost-effective approach [12]. The adsorption method can be used to

†Paper presented at the 2nd IKM Pahang Branch Symposium 2022 – Sustainability & Diversity Through Chemistry

treat the majority of dyes and their mixtures [13]. The targeted dye can be relocated from the aqueous matrix to the adsorbent surface, and this process depends on the degree of affinity of the dye towards the adsorbent. Popular adsorbents such as activated carbon, natural clay, chitosan composites, nanoparticle- and polymer-based adsorbents, as well as magnetic adsorbents have been employed to treat dye-containing wastewater and have demonstrated outstanding removal efficiency[14].

Recently, eggshell membrane (ESM) has been gaining interest in the fields of materials science, environmental science, and biotechnology [15] for its versatility as an adsorbent. ESM possesses a wide range of surface functional groups such as amines, amides, carboxylic, hydroxyl, and thiol groups, making it a very good potential adsorbent for a variety of substrates such as metals, phenols, and dyes [16]. The hydrophobic functional groups of ESM can interact with the dye's aromatic group, facilitating its removal. ESM has been employed for the adsorption of Direct Red 80 (DR80) and Acid Blue 25 (AB 25) [17], Basic Fuchsin [18], Congo Red [19], methylene blue, bromophenol blue and methyl orange [20], and malachite green [21] in aqueous solutions.

ESM can also be modified before use, and some examples include a Plantago Psyllium mucilage-ESM composite for the determination of methylene blue and methyl orange from aqueous solution [22], and an ESM-modified polyethersulfone membrane for the separation of methylene blue and sulforhodamine B dyes from sodium chloride and magnesium sulphate respectively [23]. In other studies, a CdS-TiO_2 decorated carbonized eggshell membrane (CESM) was used for the removal of methylene blue [24], a CuO/ZnO-ESM nanocomposite to adsorb Congo Red [25], a methyl-esterified eggshell membrane (MESM) to adsorb sulfur blue [26], silver nanoparticle-modified tannic acid-ESM to remove Congo Red and methyl orange [27], and magnetic eggshell membrane powder (MESM-P) to adsorb Congo Red dye from wastewater [28]. Although many different ESM-based adsorbents have been developed, to the best of the authors' knowledge none of the ESMs were modified with free fatty acids (FFAs). Gupta and Rathod proposed a similar method utilizing FFAs from waste cooking oil, although they used eggshells instead of ESM [29]. In this study, a new modified ESM adsorbent, ESM@WPCO, was developed using FFAs derived from the hydrolysis of waste palm cooking oil. The present work aimed to investigate the possibility of using ESM@WPCO for the adsorptive removal of Alizarin Red (AR) from aqueous solution. The influence of various operating parameters such as pH, adsorbent dosage, and contact time were investigated. The pseudo-first-order and pseudo-second-order models were introduced to correlate the adsorption kinetics of AR with ESM@WCPO. Langmuir and Freundlich models were used to fit the adsorption isotherms.

MATERIALS AND METHODS

Chemicals

Potassium hydroxide, *n*-hexane, and hydrochloric acid were purchased from Sigma Aldrich (Missouri, USA). Anhydrous sodium sulphate and sulphuric acid were obtained from Merck (Darmstadt, Germany), while Alizarin Red was supplied by Supelco (Bellefonte, USA). All solvents used for synthesis were analytical grade and used without further purification. Deionized water was used throughout the study. A stock solution of 100 mg L^{-1} of AR was prepared by dissolving 0.01 g of pure Alizarin Red in 100 mL deionized water. The working solutions were made daily by diluting the stock solution with deionized water to the desired concentration.

Instrumentation

FTIR spectra were recorded using a Perkin Elmer FTIR spectrophotometer (Massachusetts, USA) in the range of 4000 to 400 cm^{-1}. Surface morphological analysis of ESM and ESM@WPCO was performed using a JOEL JSM-7600F Scanning Electron Microscope (SEM, Tokyo, Japan). The adsorption study of Alizarin Red was conducted using a UV-Visible spectrophotometer (UV-Vis) (Shimadzu, Kyoto, Japan).

Preparation of ESM

Raw eggshells were collected from local eateries and immediately rinsed with deionized water to prevent decomposition. The ESM was then carefully removed from each eggshell and rinsed with deionized water again, before being dried for 1 hour at 70 °C, crushed and finally sifted with a 30 nm sieve to produce particles of consistent size.

Preparation of ESM@WPCO

ESM@WPCO (Figure 1) was prepared based on the work by Sathasivam & Haris [30] with a little modification. 0.1 g of ESM was treated with 0.5 g of filtered waste cooking oil in the presence of 5 drops of sulphuric acid as the catalyst and 10 mL of *n*-hexane. The solution was then heated for 2 hours at 60 °C. A series of ESM@WPCO were prepared with ESM:WPCO ratios of 1:1, 1:2, 1:3, 1:4, 1:5, 2:1, 3:1, and 4:1. The obtained products were washed with *n*-hexane and dried under vacuum at 70 °C for 24 hours to yield the final products.

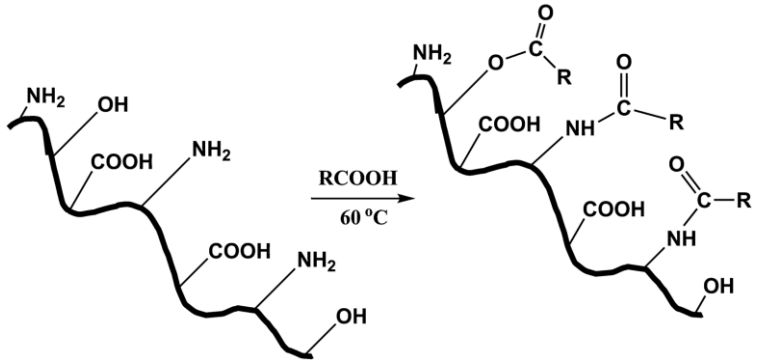

Figure 1. Schematic diagram of the preparation of ESM@WPCO

Adsorption Experiments

The adsorption experiments began by mixing ESM@WPCO with 15 mL of AR solution. The mixture was then agitated at 150 rpm at ambient temperature for 10 to 40 minutes. Then, the adsorbent was filtered and the residual concentration was evaluated using a UV-Vis spectrophotometer at a wavelength of 405 nm. All experiments were conducted in triplicate. The percentage of removal, R (%), was calculated using equation 1, where C_0 and C_f are the initial and residual concentrations of AR (mg L^{-1}) in the solution.

$$R(\%) = \frac{C_0 - C_f}{C_0} \times 100\% \quad (1)$$

The effects of adsorbent dosage, pH, reaction time, and initial concentration were studied in detail using a one-factor-at-a-time method. The AR removal efficiency was initially examined using five different adsorbent dosages (5, 10, 20, 40 and 60 mg). The initial concentration of AR was fixed at 50 mg L^{-1} at pH 2 and 40 min of treatment time. The pH effect was then investigated using a pH range of 2-10. The effect of treatment time was evaluated at different intervals of 10-70 min at room temperature. The initial AR concentration was fixed at 50 mg L^{-1} with an adsorbent dosage of 20 mg at pH 2. The effect of the initial concentration of AR dye was investigated at 20, 50, 60 and 80 mg L^{-1} using the optimized parameters: 20 mg of adsorbent, 40 min of treatment time, and pH 2.

Adsorption Kinetics and Isotherm Study

An adsorption kinetics experiment was carried out at 10–60 min intervals using the optimized parameters as previously described. The adsorption isotherm experiment was carried out using different initial AR concentrations (20, 50, 80 and 100 mg L^{-1}). The pseudo-first-order and pseudo-second-order models were used in an attempt to fit the adsorption kinetics, while the Langmuir and Freundlich models were used in an attempt to fit the adsorption isotherm data. The residual concentration of AR in the supernatant solution was determined, and the adsorption capacity, i.e., the amount of AR adsorbed per unit mass of the adsorbent (q_e) was calculated using equation 2:

$$q_e = \frac{(C_0 - C_e)V}{W} \quad (2)$$

where C_0 and C_e are the initial and equilibrium concentrations of solution (mg L^{-1}), respectively, while V (L) is the volume of the solution and W (g) is the mass of the dry adsorbent used.

RESULTS AND DISCUSSION

1. Characterization of ESM and ESM@WPCO

Figure 2 shows the characteristic bands for the functional groups present in (A) unmodified ESM and (B) ESM@WPCO (using a 1:5 ratio of ESM:WPCO). There are significant differences between the characteristic peaks for both adsorbents. For the unmodified ESM, a strong broad band was present at 3299.45 cm^{-1} which is associated with the presence of O-H and N-H groups (Figure 2A). Other important peaks were located at 1649.67 cm^{-1} corresponding to the carbonyl group, 1528.48 cm^{-1} corresponding to N-H bending, 1400.9 cm^{-1} corresponding to C-H bending, and 1237.4 cm^{-1} corresponding to C-O stretching. After functionalization with free fatty acids, new distinctive peaks appeared at 2925.7 cm^{-1} and 2855.6 $cm^{-1,}$ which correspond to the stretching of the asymmetric and symmetric CH_2 [31,32]. The presence of these new bands in Figure 2B suggests that the free fatty acids were successfully functionalized onto the ESM.

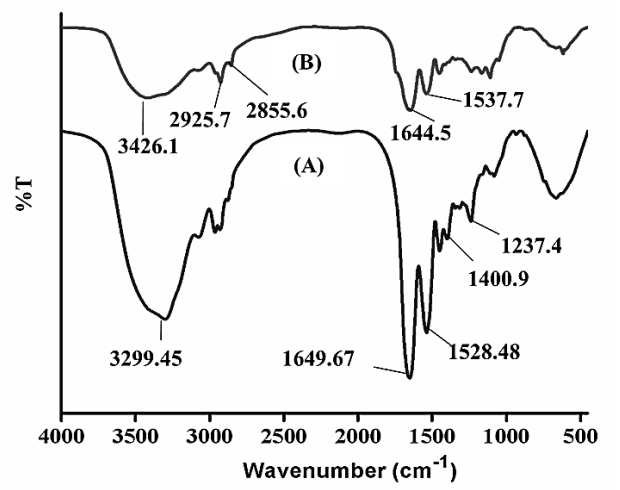

Figure 2. FT-IR spectrum (A) ESM (B) ESM@WPCO

Morphological analysis was performed using SEM to determine the surface features of ESM@WPCO. The image in Figure 3 was captured at a magnification of 500x. The ESM@WPCO was observed to consist of a highly porous network of interweaving and coalescing shell membrane fibres. The porous structure provides a high surface area for AR adsorption onto the ESM@WPCO surface.

2. Optimization of the Eggshell Membrane (ESM) to Waste Palm Cooking Oil (WPCO) Mass Ratio

The mass ratio of ESM to WPCO was varied to evaluate the AR dye removal performance of ESM@WPCO (Figure 4). The percentage of AR removal was 78% at a mass ratio of 1:1 ESM: WPCO. The AR removal increased progressively as the mass of WPCO was increased, reaching a maximum of 92% at 1:5 ESM:WPCO. The increase of WPCO contributed to the increase of hydrophobic sites at ESM@WPCO, and therefore the active sites for the adsorption of AR. At the optimum mass ratio of 1:5 ESM:WPCO, it can be reasonably expected that hydrogen bonding and hydrophobic interactions occur synergistically to bind AR at the surface of the ESM@WPCO. Conversely, when the mass of WPCO was reduced, the percentage removal of AR also decreased. The relative decrease in WPCO reduced the available hydrophobic interactions between the aromatic core of the AR and the ESM@WPCO. Therefore, the optimum mass ratio of 1:5 ESM:WPCO was selected and used in subsequent experiments.

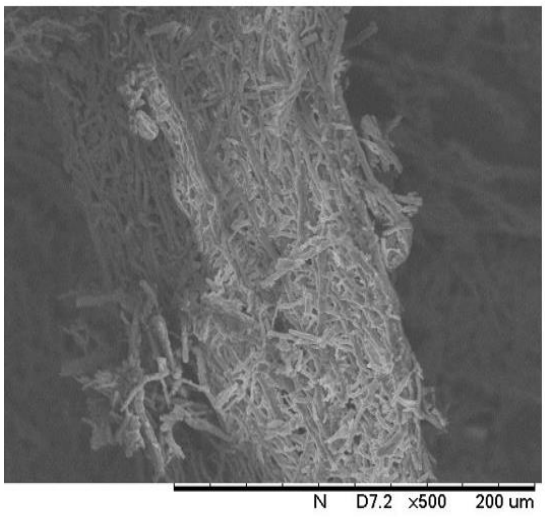

Figure 3. SEM image of ESM@WPCO.

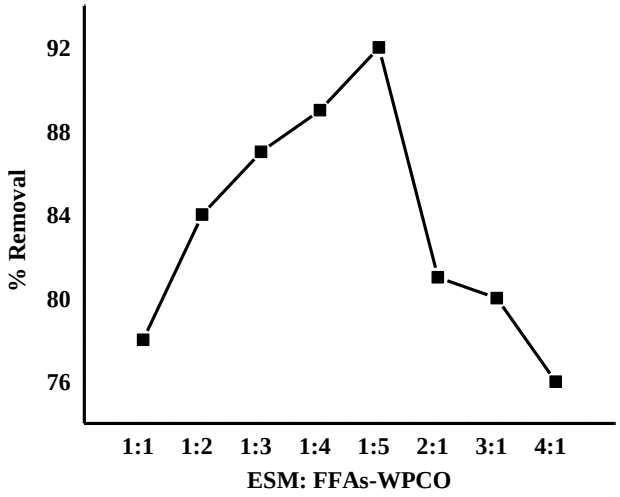

Figure 4. Percentage of AR removal against ESM@WPCO mass ratio

3. Comparative AR Dye Removal Performance of ESM and ESM@WPCO

A comparative screening was conducted to evaluate the performance of ESM and ESM@WPCO (using a 1:5 ratio of ESM:WPCO) in AR dye removal. Preliminary investigation showed that the adsorption process of AR occurred at both ESM and ESM@WPCO surfaces. Under identical conditions, the percentage of AR removal by ESM and ESM@WPCO were 44% and 87%, respectively. The adsorption of AR onto ESM is governed only by hydrogen bonding between the oxygen of the carbonyl group from the AR ring and the hydrogen of the NH_2 and OH groups at the surface of the ESM. The functionalization of WPCO onto ESM enables the hydrophobic interaction between AR and ESM@WPCO through the aromatic core of the AR structure and the R group (amide) at the adsorbent surface. The improved performance of ESM@WPCO is due to its hydrophobic interaction and hydrogen bonding with AR. The interactions between AR and ESM@WPCO are illustrated in Figure 5.

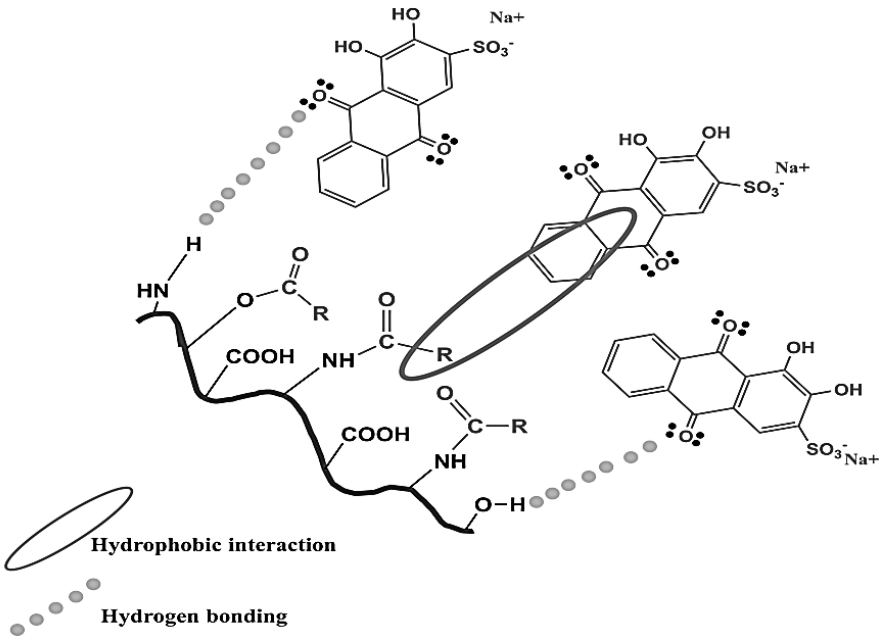

Figure 5. Interactions that occur between AR dye and ESM@WPCO

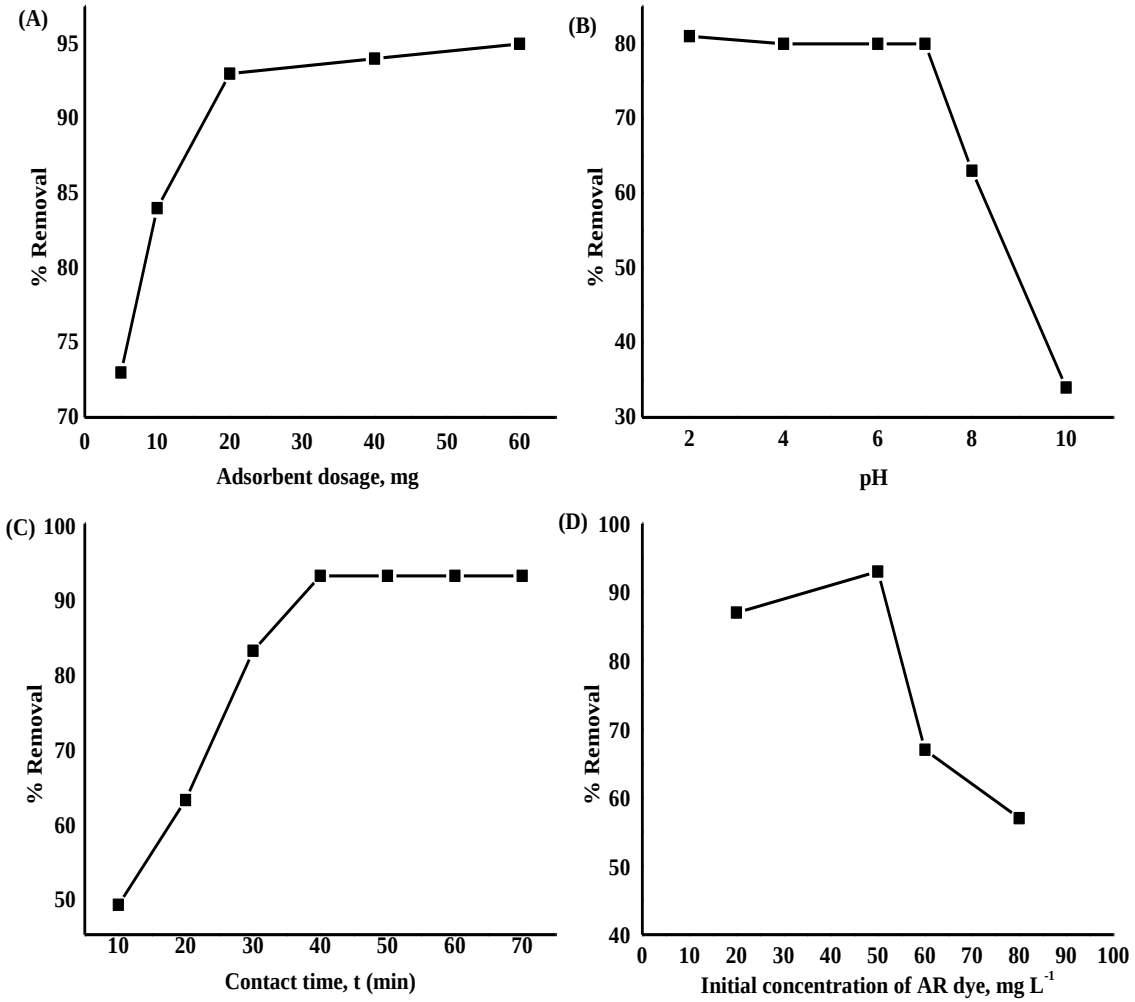

Figure 6. Effects of **(A)** adsorbent dosage (pH2, 50 mg L^{-1} AR, 40 min) **(B)** pH (50 mg L^{-1} AR, 40 min, 20 mg ESM@WPCO), **(C)** contact time (pH2, 50 mg L^{-1} AR, 20 mg ESM@WPCO) and **(D)** initial concentration of AR dye (pH2, 40 min, 20 mg ESM@WPCO), on the removal of AR dye

4. Optimization of Operating Parameters for AR Removal

4.1. Effect of Adsorbent Dosage

Figure 6(A) shows the influence of adsorbent dosage on the removal of AR dye. Five different amounts of ESM@WPCO (5, 10, 20, 40, 60 mg) were used to adsorb 50 mg L^{-1} of AR dye from 15 mL of deionized water. As the adsorbent dosage was increased to 20 mg, AR adsorption was found to increase significantly, due to the increase in the available sorbent surface area and therefore sorption sites. When the dosage of ESM@WPCO exceeded 20 mg, the curve started to taper off, as the adsorbed AR concentration and free AR reached equilibrium [33]. This is because there were more available active sites for adsorption than free AR molecules in the solution [34]. The percentage of AR removal increased from 73% to 93% when the adsorbent dose was increased from 5 to 20 mg. Therefore, 20 mg of adsorbent was used in subsequent experiments.

4.2. Effect of pH

The functional group of the adsorbent and adsorbate may be protonated and deprotonated depending on the pH of the solution, and this affects electrostatic interactions between the materials. Figure 6(B) shows the percentage of AR removal at different pH values. The results show that the adsorption process was strongly pH dependent, and AR removal increased as the pH value decreased. A maximum AR removal of 81% was obtained at pH 2. Fayazi et al. [35] explained that the adsorption phenomenon was based on the electrostatic interaction between the dye molecules with the residual (non-functionalized) amino group of the adsorbent. Under acidic conditions, the residual

amino, carboxylic acid and hydroxyl groups of the adsorbent are protonated as described in the following equations:

$$R - NH_2 + H^+ \leftrightarrow R - NH_3{}^+ \quad (3)$$

$$R - COOH + H^+ \leftrightarrow R - COOH_2^+ \quad (4)$$

$$R - OH + H^+ \leftrightarrow R - OH_2^+ \quad (5)$$

AR is an anionic dye due to its negatively charged sulfonate groups ($-SO_3^-$) in aqueous solution. The dissociation of AR dye in aqueous solution is shown as follows:

$$D - SO_3Na \leftrightarrow D - SO_3{}^- + Na^+ \quad (6)$$

Therefore, the adsorption of AR proceeds through an electrostatic interaction as shown below [36]:

$$R - NH_3{}^+ + D - SO_3^- \leftrightarrow R - NH_3^+ \ldots SO_3D \quad (7)$$

At pH 2, the residual amines are in protonated form and therefore preferable for the adsorption of the AR dye. Colour removal was found to decrease at pH values higher than 7, down to 34% at pH 10. This phenomenon is due to the decrease in protonation of the residual $–NH_2$, –OH, and –COOH, and the increase in –OH groups that compete with the anionic sulphonic groups for the active sites. The high pH promotes electrostatic repulsion between the AR dye molecules and the negatively-charged surface of ESM@WPCO, causing a decrease in its adsorption capacity. The results obtained here agree with the findings published by Celekli et al. [37], Gupta et al. [38] and Gautam et al. [39]. The effects of acidic and basic media on the AR adsorption process are illustrated in Figure 7. pH 2 was selected as the optimum pH for AR dye removal in aqueous solution and used in subsequent experiments.

4.3. Effect of Treatment Time

Figure 6(C) describes the percentage removal of AR as a function of treatment time. The percentage of AR removed increased as the treatment duration increased. AR sorption increased rapidly for the first 40 minutes, then slowed down and reached equilibrium after 70 minutes. The highest percentage of AR removed was 93% after 40 min of treatment time. In the first 40 min, rapid distribution of AR from the solution to the large surface area of ESM@WPCO occurred [35,40]. However, as more sites became occupied, the adsorption efficiency decreased as it became harder for the AR to find a free sorption site. Therefore, 40 minutes was the optimum contact time for the removal of AR using ESM@-WPCO and this value was used in subsequent experiments.

4.4. Effect of Initial AR Concentration

The removal of AR dye by ESM@WPCO was dependent on its initial concentration (Figure 6(D)). The variation in AR uptake with different initial dye concentrations (20 – 80 mg L^{-1}) was investigated. An increase in initial AR dye concentration from 20 to 50 mg L^{-1} led to an increased dye uptake by the adsorbents. The highest removal rate was observed when 50 mg L^{-1} of AR dye was used. At higher concentration rates (60 and 80 mg L^{-1}), uptake was reduced due to dye particle accumulation at the sorption sites, resulting in a decrease in sorption. It is known that the availability of adsorption sites is a limiting factor for the dye sorption process [35]. Therefore, an initial concentration of 50 mg L^{-1} of AR dye in aqueous solution was used in subsequent experiments.

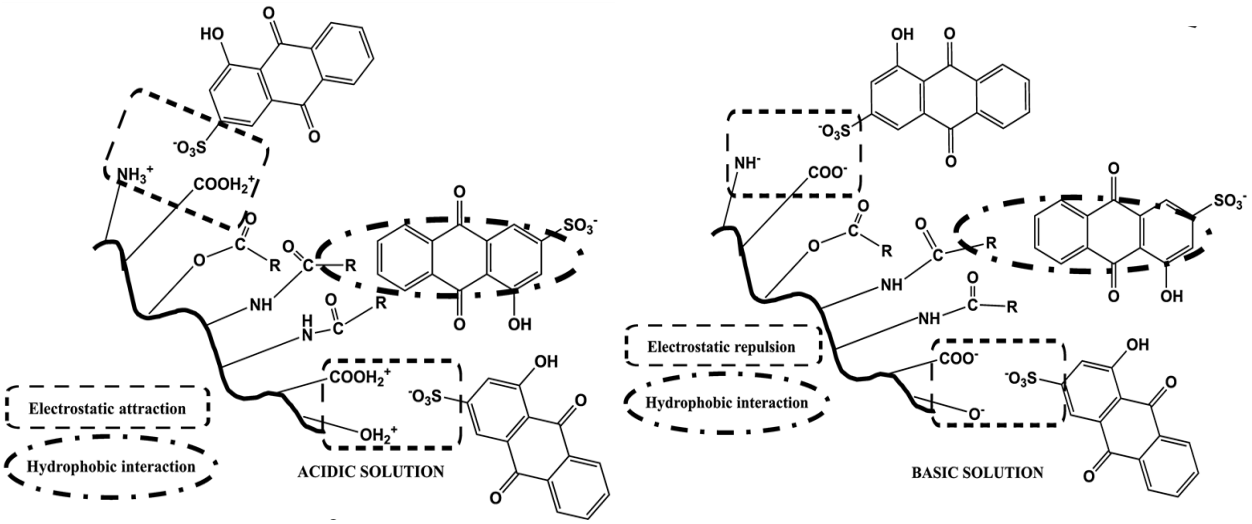

Figure 7. Interactions between Alizarin Red dye and ESM@WPCO in acidic and basic solutions.

5. Adsorption Kinetics

Pseudo-first-order and pseudo-second-order models were employed to fit the adsorption process of AR onto ESM@WPCO. The pseudo-first-order model is a simple kinetic evaluation of the equilibrium established between the liquid phase and the sorbent. This model proposes that initially, there is no sorbate present, but with time, sorbate ions accumulate on the surface of the sorbent [36]. The pseudo-first order equation is provided as equation 8:

$$\log(q_e - q_t) = log q_e - \frac{k_1 t}{2.303} \quad (8)$$

where q_e and q_t are the adsorbed amounts (mg) of AR at equilibrium and at time t (min), respectively, and k_1 (min^{-1}) is a constant adsorption rate. The log (q_e - q_t) against t was plotted, and the slope of the graph gave the value of the k_1 (Figure 7A). Table 1 summarizes the kinetic parameters for AR dye adsorption on the ESM@WPCO. It was observed that the correlation coefficient (R^2) had a low value of <0.96. There was a very large difference between q (experimental) and q (calculated); therefore, the pseudo-first-order model did not fit the experimental data.

The pseudo-second order model is provided as equation 9:

$$\frac{t}{q_t} = \frac{1}{k_2 q_e^2} + \frac{1}{q_e} t \quad (9)$$

where k_2 (g mg^{-1} min^{-1}) is the rate constant determined from the slope of t/q_t versus t. It can be seen in Figure 7(B) that the linear correlation coefficient value R^2 was 0.99. The pseudo-second-order constant, k_2 and the adsorption equilibrium, q_e values were found to be 0.0014 g mg^{-1} min^{-1} and 45.45 mg g^{-1}, respectively. The q_e value was similar to the value obtained from the experiment indicating that the sorption system followed the second-order kinetics model. Therefore, it can be concluded that the adsorption of AR onto ESM@WPCO followed the chemisorption mechanism, driven by a chemical reaction that occurs on the adsorbent's surface [41].

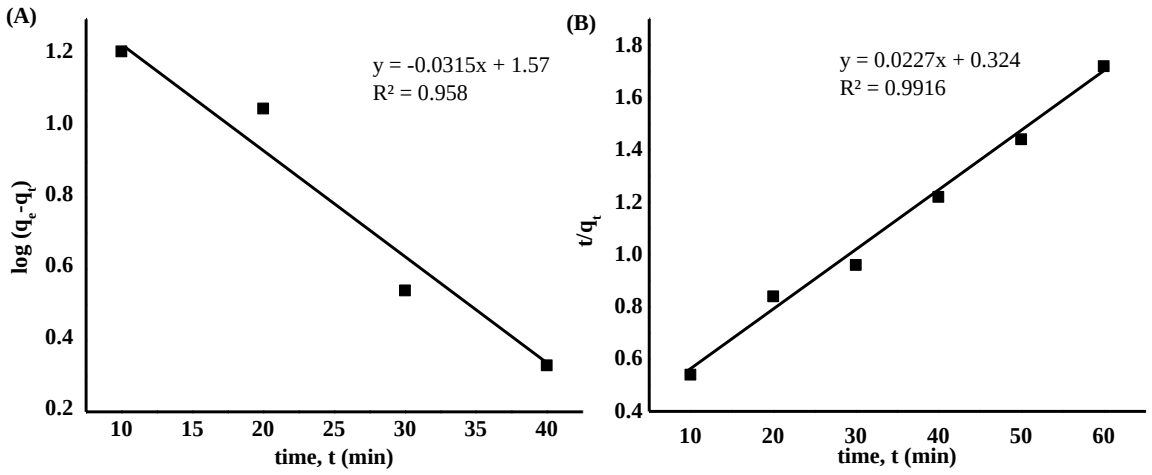

Figure 8. (A) Pseudo-first order kinetics and (B) pseudo-second order kinetics of Alizarin Red dye adsorption on ESM@WPCO.

Table 1. Kinetic parameters for AR dye adsorption on the ESM@WPCO adsorbent.

Pseudo-first-order			Pseudo-second-order		
k_1 (min^{-1})	q_e (mg g^{-1})	R^2	k_2 (g mg^{-1} min^{-1})	q_e (mg g^{-1})	R^2
7.729	37.15	0.958	0.0014	45.45	0.9916

6. Evaluation of the Adsorption Isotherm Models

The adsorption behaviour of AR onto ESM@WPCO was analyzed using the Freundlich and Langmuir adsorption isotherm models. The Langmuir isotherm assumes homogeneous adsorption, while the Freundlich isotherm assumes heterogenic adsorption [42]. The Langmuir model can be expressed as equation 10:

$$\frac{c_e}{q_e} = \frac{1}{k_l q_m} + \frac{1}{q_m} c_e \qquad (10)$$

where c_e is the equilibrium concentration of the dye solution (mg L^{-1}), q_e is the adsorption capacity at equilibrium (mg g^{-1}), k_1 is the constant related to the free energy of adsorption (L mg^{-1}), and q_m is the maximum adsorption capacity at monolayer coverage (mg g^{-1}). Figure 9(A) shows the plot of q_e against C_e. Table 2 summarizes the adsorption isotherm parameters for AR dye adsorption on the ESM@WPCO adsorbent. The value of q_m and k_1 were found to be 50.0 and 0.129, respectively.

Equation 11 is the equation for the Freundlich model:

$$q_e = k_f c_e^{1/n} \qquad (11)$$

where $k_f (mg^{1-\frac{1}{n}} L^{\frac{1}{n}} g^{-1})$ is the Freundlich constant and n represents the adsorption capacity and adsorption intensity. The plot of ln q_e against ln c_e (Figure 9B) was constructed, and the k_f and n values obtained from the slope and intercept were 8.41 g mg^{-1} and 2.31, respectively. The theoretical q_e was comparable with the obtained q_e from the experiment because the exponent was between $1< n <10$. By comparing the R^2 values of the two isotherm models, it was clear that the Freundlich model better explained the adsorption of AR onto the ESM@WPCO surface. The n value indicated that the adsorption process was a chemical process.

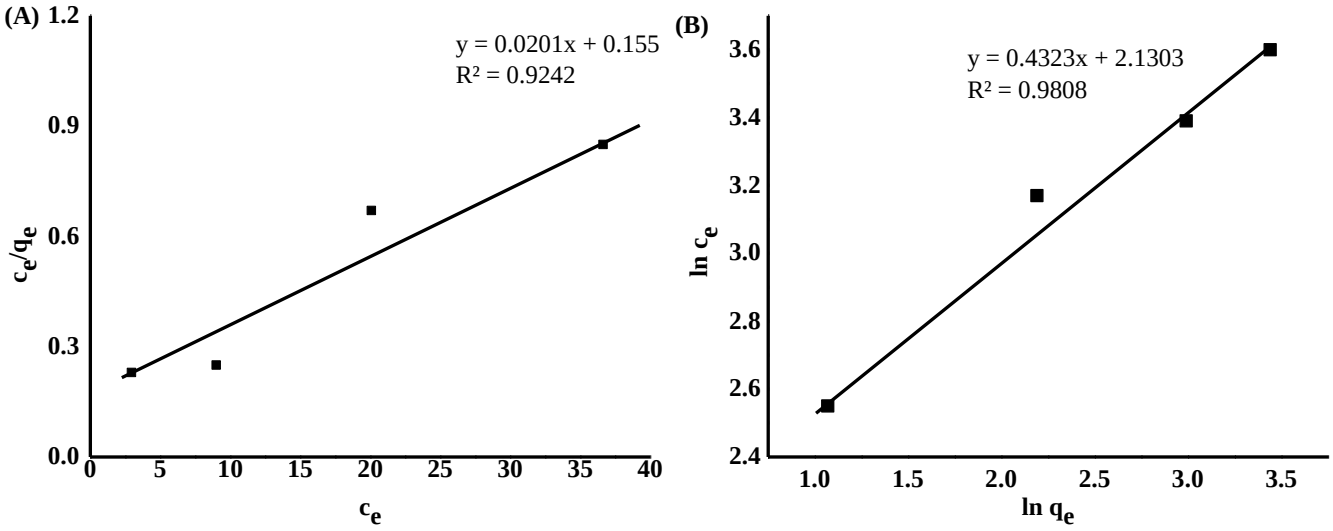

Figure 9. (A) Langmuir isotherm and (B) Freundlich isotherm of Alizarin Red dye adsorption on ESM@WPCO

Table 2. Adsorption isotherm parameters for AR dye adsorption on the ESM@WPCO adsorbent

Langmuir isotherm			Freundlich isotherm		
k_1 (L mg^{-1})	q_m (mg g^{-1})	R^2	k_f (mg^{1+n}/gL^n)	n	R^2
0.129	50.0	0.9242	8.41	2.31	0.9808

CONCLUSION

ESM@WPCO was synthesized, characterized, and evaluated for its ability to adsorb AR. ESM@-WPCO exhibited better adsorption capacity for AR than ESM. The adsorption of AR was preferred under acidic conditions. The adsorption of AR onto ESM@WPCO fit the pseudo-second-order model and the Freundlich model well. The adsorption mechanism could be attributed to the electrostatic effect, hydrogen bonding and hydrophobic interactions between AR and the functional groups on ESM@WPCO. The results presented in this paper show that ESM@WPCO is a viable, low-cost adsorbent for the effective removal of AR dye from aqueous solutions. However, more research is needed to investigate the performance of ESM@WPCO in real wastewater applications.

ACKNOWLEDGEMENT

This study was supported by the Special Research Grant (600-RMC/GPK 5/3 (181/2020) from Universiti Teknologi MARA.

CONFLICT OF INTEREST

The authors declare that they have no known competing financial interests or personal relationships that could have appeared to influence the work reported in this paper.

REFERENCES

1. Fan, L., Zhang, Y., Li, X., Luo, C., Lu, F. and Qiu, H. (2012) Removal of alizarin red from water environment using magnetic chitosan with Alizarin Red as imprinted molecules. *Colloids and Surfaces B: Biointerfaces*, **91**, 250–257. https://doi.org/10.1016/j.colsurfb.2011.11.014

2. Hessel, C., Allegre, C., Maisseu, M., Charbit, F. and Moulin, P. (2007) Guidelines and legislation for dye house effluents. *Journal of Environmental Management*, **83(2)**, 171–180. https://doi.org/10.1016/j.jenvman.2006.02.012

3. Liu, M., Zhang, X., Li, Z., Qu, L. and Han, R. (2020) Fabrication of zirconium (IV)-loaded chitosan/Fe3O4/graphene oxide for efficient removal of alizarin red from aqueous solution, *Carbohydrate Polymers*, **248**, 116792. https://doi.org/10.1016/j.carbpol.2020.116792

4. Routoula, E. and Patwardhan, S. V. (2020) Degradation of Anthraquinone Dyes from Effluents: A Review Focusing on Enzymatic Dye Degradation with Industrial Potential. *Environmental Science & Technology*, **54(2)**, 647–664. https://doi.org/10.1021/acs.est.9b03737

5. Christie, R. (2014) *Colour Chemistry*, Royal Society of chemistry, United Kingdom.

6. Khehra, M. S., Saini, H. S., Sharma, D. K., Chadha, B. S. and Chimni, S. S. (2006) Biodegradation of azo dye C.I. Acid Red 88 by an anoxic–aerobic sequential bioreactor. *Dyes and Pigments*, **70(1)**, 1–7. https://doi.org/10.1016/j.dyepig. 2004.12.021

7. Popli, S. and Patel Upendra, D. (2015) Destruction of azo dyes by anaerobic–aerobic sequential biological treatment: a review. *International Journal of Environmental Science and Technology*, **12(1)**, 405–420. https://doi.org/10.1007/s13762-014-0499-x

8. Zucca, P., Vinci, C., Sollai, F., Rescigno, A. and Sanjust, E. (2008) Degradation of Alizarin Red S under mild experimental conditions by immobilized 5,10,15,20-tetrakis(4-sulfonatophenyl)porphine–Mn(III) as a biomimetic peroxidase-like catalyst. *Journal of Molecular Catalysis A: Chemical*, **288(1–2)**, 97–102. https://doi.org/10.1016/j.molcata.2008.04.001

9. Gholivand, M. B., Yamini, Y., Dayeni, M., Seidi, S. and Tahmasebi, E. (2015) Adsorptive removal of alizarin red-S and alizarin yellow GG from aqueous solutions using polypyrrole-coated magnetic nanoparticles. *Journal of Environmental Chemical Engineering*, **3(1)**, 529–540. https://doi.org/10.1016/j.jece.2015.01.011

10. Machado, F. M., Carmalin, S. A., Lima, E. C., Dias, S. L. P., Prola, L. D. T., Saucier, C., Jauris, I. M., Zanella, I. and Fagan, S. B. (2016) Adsorption of Alizarin Red S Dye by Carbon Nanotubes: An Experimental and Theoretical Investigation. *The Journal of Physical Chemistry C*, **120(32)**, 18296–18306. https://doi.org/10.1021/acs.jpcc.6b03884

11. Adane, T., Adugna, A. T. and Alemayehu, E. (2021), Textile Industry Effluent Treatment Techniques. *Journal of Chemistry*, **2021**, 1–14. https://doi.org/10.1155/2021/5314404

12. Xu, J., Cao, Z., Zhang, Y., Yuan, Z., Lou, Z., Xu, X. and Wang, X. (2018) A review of functionalized carbon nanotubes and graphene for heavy metal adsorption from water: Preparation, application, and mechanism. *Chemosphere*, **195**, 351–364. https://doi.org/10.1016/j.chemosphere.2017.12.061

13. Delpiano, G. R., Tocco, D., Medda, L., Magner, E. and Salis, A. (2021) Adsorption of Malachite Green and Alizarin Red S Dyes Using Fe-BTC

Metal Organic Framework as Adsorbent. *International Journal of Molecular Sciences*, **22(2)**, 788. https://doi.org/10.3390/ijms22020788

14. Kubra, K. T., Salman, Md. S. and Hasan, Md. N. (2021) Enhanced toxic dye removal from wastewater using biodegradable polymeric natural adsorbent. *Journal of Molecular Liquids*, **328**, 115468. https://doi.org/10.1016/j.molliq.2021.115468

15. Liu, B. and Huang, Y. (2011) Polyethyleneimine modified eggshell membrane as a novel biosorbent for adsorption and detoxification of Cr(VI) from water. *Journal of Materials Chemistry*, **21(43)**, 17413. https://doi.org/10.1039/c1jm12329g

16. Al-Ghouti, M. A. and Khan, M. (2018) Eggshell membrane as a novel bio sorbent for remediation of boron from desalinated water. *Journal of Environmental Management*, **207**, 405–416. https://doi.org/10.1016/j.jenvman.2017.11.062

17. Arami, M., Yousefi Limaee, N. and Mahmoodi, N. M. (2006) Investigation on the adsorption capability of egg shell membrane towards model textile dyes. *Chemosphere*, **65(11)**, 1999–2008. https://doi.org/10.1016/j.chemosphere.2006.06.074

18. Bessashia, W., Berredjem, Y., Hattab, Z. and Bououdina, M. (2020) Removal of Basic Fuchsin from water by using mussel powdered eggshell membrane as novel bioadsorbent: Equilibrium, kinetics, and thermodynamic studies. *Environmental Research*, **186**, 109484. https://doi.org/10.1016/j.envres.2020.109484

19. Parvin, S., Biswas, B. K., Rahman, M. A., Rahman, M. H., Anik, M. S. and Uddin, M. R. (2019) Study on adsorption of Congo red onto chemically modified egg shell membrane. *Chemosphere*, **236**, 124326. https://doi.org/10.1016/j.chemosphere.2019.07.057

20. Salman, D. D., Ulaiwi, W. S. and Tariq, N. M. (2012) Determination the optimal conditions of methylene blue adsorption by the chicken Egg Shell Membrane. *International Journal of Poultry Science*, **11(6)**, 391–396.

21. Chen, H. M., Liu, J., Cheng, X. Z. and Peng, Y. (2012) Adsorption for the Removal of Malachite Green by Using Eggshell Membrane in Environment Water Samples. *Advanced Materials Research*, **573–574**, 63–67. https://doi.org/10.4028/www.scientific.net/AMR.573-574.63

22. Mirzaei, S. and Javanbakht, V. (2019) Dye removal from aqueous solution by a novel dual cross-linked biocomposite obtained from mucilage of Plantago Psyllium and eggshell membrane. *International Journal of Biological Macromolecules*, **134**, 1187–1204. https://doi.org/10.1016/j.ijbiomac.2019.05.119

23. Sundarajan, S., Sriram, K., Gangasalam, A., Kweon, J. and Ismail, A. F. (2021) Effective separation of salts and dye using egg shell membrane (ESP) incorporated polyethersulfone polymer material. *Emergent Materials*, **4(5)**, 1413–1423. https://doi.org/10.1007/s42247-020-00137-7

24. Pant, B., Park, M., Kim, H.-Y. and Park, S.-J. (2017) CdS-TiO_2 NPs decorated carbonized eggshell membrane for effective removal of organic pollutants: A novel strategy to use a waste material for environmental remediation. *Journal of Alloys and Compounds*, **699**, 73–78. https://doi.org/10.1016/j.jallcom.2016.12.360

25. He, X., Yang, D.-P., Zhang, X., Liu, M., Kang, Z., Lin, C., Jia, N. and Luque, R. (2019) Waste eggshell membrane-templated CuO-ZnO nanocomposites with enhanced adsorption, catalysis and antibacterial properties for water purification. *Chemical Engineering Journal*, **369**, 621–633. https://doi.org/10.1016/j.cej.2019.03.047

26. Choi, H.-J. (2017) Use of methyl esterified eggshell membrane for treatment of aqueous solutions contaminated with anionic sulfur dye. *Water Science and Technology*, **76(10)**, 2638–2646. https://doi.org/10.2166/wst.2017.346

27. Liu, X., Liang, M., Liu, M., Su, R., Wang, M., Qi, W. and He, Z. (2016) Highly Efficient Catalysis of Azo Dyes Using Recyclable Silver Nanoparticles Immobilized on Tannic Acid-Grafted Eggshell Membrane. *Nanoscale Research Letters*, **11(1)**, 440. https://doi.org/10.1186/s11671-016-1647-7

28. Zhao, J., Wen, X., Xu, H., Weng, Y. and Chen, Y. (2021) Fabrication of recyclable magnetic biosorbent from eggshell membrane for efficient adsorption of dye. *Environmental Technology*, **42(28)**, 4380–4392. https://doi.org/10.1080/09593330.2020.1760355

29. Gupta, A. R. and Rathod, V. K. (2018) Waste cooking oil and waste chicken eggshells derived solid base catalyst for the biodiesel production: Optimization and kinetics. *Waste Management*,

79, 169–178. https://doi.org/10.1016/j.wasman.2018.07.022

30. Sathasivam, K. and Mas Haris, M. R. H. (2010) Adsorption Kinetics and Capacity of Fatty Acid-Modified Banana Trunk Fibers for Oil in Water. *Water, Air, & Soil Pollution*, **213(1–4)**, 413–423. https://doi.org/10.1007/s11270-010-0395-z

31. Ibarra, J., Melendres, J., Almada, M., Burboa, M. G., Taboada, P., Juárez, J. and Valdez, M. A. (2015) Synthesis and characterization of magnetite/PLGA/chitosan nanoparticles. *Materials Research Express*, **2(9)**, 095010. https://doi.org/10.1088/2053-1591/2/9/095010

32. Matwijczuk, A., Zając, G., Karcz, D., Chruściel, E., Matwijczuk, A., Kachel-Jakubowska, M., Łapczyńska-Kordon, B. and Gagoś, M. (2018) Spectroscopic studies of the quality of WCO (Waste Cooking Oil) fatty acid methyl esters. *BIO Web of Conferences*, **10**, 02019. https://doi.org/10.1051/bioconf/20181002019

33. Boudrahem, F., Aissani-Benissad, F. & Soualah, A. (2011) Adsorption of Lead(II) from Aqueous Solution by Using Leaves of Date Trees As an Adsorbent. *Journal of Chemical & Engineering Data*, **56(5)**, 1804–1812. https://doi.org/10.1021/je100770j

34. Kuang, Y., Zhang, X. and Zhou, S. (2020) Adsorption of Methylene Blue in Water onto Activated Carbon by Surfactant Modification. *Water*, **12(2)**, 587. https://doi.org/10.3390/w12020587

35. Fayazi, M., Ghanei-Motlagh, M. & Taher, M. A. (2015) The adsorption of basic dye (Alizarin red S) from aqueous solution onto activated carbon/γ-Fe2O3 nano-composite: Kinetic and equilibrium studies. *Materials Science in Semiconductor Processing*, **40**, 35–43. https://doi.org/10.1016/j.mssp.2015.06.044

36. Zhou, L., Jin, J., Liu, Z., Liang, X. Shang, C. (2011) Adsorption of acid dyes from aqueous solutions by the ethylenediamine-modified magnetic chitosan nanoparticles. *Journal of Hazardous Materials*, **185(2–3)**, 1045–1052. https://doi.org/10.1016/j.jhazmat.2010.10.012

37. Çelekli, A., Birecikligil, S. S., Geyik, F. and Bozkurt, H. (2012) Prediction of removal efficiency of Lanaset Red G on walnut husk using artificial neural network model. *Bioresource Technology*, **103(1)**, 64–70. https://doi.org/10.1016/j.biortech.2011.09.106

38. Gupta, V. K., Rastogi, A. and Nayak, A. (2010) Adsorption studies on the removal of hexavalent chromium from aqueous solution using a low cost fertilizer industry waste material. *Journal of Colloid and Interface Science*, **342(1)**, 135–141. https://doi.org/10.1016/j.jcis.2009.09.065

39. Gautam, R. K., Gautam, P. K., Chattopadhyaya, M. C. and Pandey, J. D. (2014) Adsorption of Alizarin Red S onto Biosorbent of Lantana camara: Kinetic, Equilibrium Modeling and Thermodynamic Studies. *Proceedings of the National Academy of Sciences, India Section A: Physical Sciences*, **84(4)**, 495–504. https://doi.org/10.1007/s40010-014-0154-4

40. Katha, P. S., Ahmed, Z., Alam, R., Saha, B., Acharjee, A. and Rahman, M. S. (2021) Efficiency analysis of eggshell and tea waste as Low cost adsorbents for Cr removal from wastewater sample. *South African Journal of Chemical Engineering*, **37**, 186–195. https://doi.org/10.1016/J.SAJCE.2021.06.001

41. Kumar, P. S., Vincent, C., Kirthika, K. and Kumar, K. S. (2010) Kinetics and equilibrium studies of Pb2+ in removal from aqueous solutions by use of nano-silversol-coated activated carbon. *Brazilian Journal of Chemical Engineering*, **27(2)**, 339–346. https://doi.org/10.1590/S0104-66322010000200012

42. Zolgharnein, J., Asanjrani, N., Bagtash, M. and Azimi, G. (2014) Multi-response optimization using Taguchi design and principle component analysis for removing binary mixture of alizarin red and alizarin yellow from aqueous solution by nano γ-alumina. *Spectrochimica Acta Part A: Molecular and Biomolecular Spectroscopy*, **126**, 291–300. https://doi.org/10.1016/j.saa.2014.01.100.